

See discussions, stats, and author profiles for this publication at: <https://www.researchgate.net/publication/231532125>

# Photoinduced Electron Transfer in Phytochlorin –[60]Fullerene Dyads

ARTICLE *in* JOURNAL OF THE AMERICAN CHEMICAL SOCIETY · SEPTEMBER 1999

Impact Factor: 12.11 · DOI: 10.1021/ja9915605

CITATIONS

240

READS

21

6 AUTHORS, INCLUDING:



**Nikolai Tkachenko**

Tampere University of Technology

267 PUBLICATIONS 4,559 CITATIONS

SEE PROFILE



**Paavo Heikki Hynninen**

University of Helsinki

91 PUBLICATIONS 1,877 CITATIONS

SEE PROFILE



**Helge Lemmetyinen**

Tampere University of Technology

422 PUBLICATIONS 6,385 CITATIONS

SEE PROFILE

## Photoinduced Electron Transfer in Phytochlorin–[60]Fullerene Dyads

Nikolai V. Tkachenko,<sup>\*,†</sup> Lasse Rantala,<sup>†</sup> Andrei Y. Tauber,<sup>†,‡</sup> Juho Helaja,<sup>‡</sup>  
Paavo H. Hynninen,<sup>‡</sup> and Helge Lemmetyinen<sup>†</sup>

Contribution from the Institute of Materials Chemistry, Tampere University of Technology, P.O. Box 541, FIN-33101 Tampere, Finland, and Department of Chemistry, University of Helsinki, P.O. Box 55, FIN-00014 Helsinki, Finland

Received May 10, 1999. Revised Manuscript Received August 3, 1999

**Abstract:** Novel molecular electron donor–acceptor (DA) dyads, composed of a phytochlorin donor and a [60]fullerene acceptor, have been photochemically characterized. In these dyads, a pyrrolidine spacer group links the chlorin and the C<sub>60</sub> moieties covalently, forming a rigid dyad with a short and almost constant D–A distance. The photochemical behavior of the metal-free dyads and the corresponding Zn complexes was studied by means of fluorescence and absorption spectroscopies with femto- and picosecond time resolutions in polar benzonitrile and nonpolar toluene solutions. In consistence with the previous studies on porphyrin–fullerene dyads, the novel chlorin–fullerene dyads underwent a fast intramolecular photoinduced electron transfer in a benzonitrile solution. The recombination rates of the charge-transfer (CT) states were  $4.8 \times 10^{10} \text{ s}^{-1}$  for the Zn dyads and ca.  $1.5 \times 10^{10} \text{ s}^{-1}$  for the metal-free compounds. The CT state was preceded by at least three intermediate states in the time domain from 200 fs to 100 ps. Two of the states were identified as singlet excited states of either the phytochlorin or the fullerene moiety. The third state was attributed to an intramolecular exciplex, which was transformed to the CT state. In the frame of this model, the formation rate constant of the CT state was estimated to be  $1.6 \times 10^{11} \text{ s}^{-1}$  for the Zn dyads and  $0.5 \times 10^{11} \text{ s}^{-1}$  for the metal-free compounds. The formation of the exciplex was also observed in nonpolar solvents, e.g., toluene. In contrast to the behavior in polar solvents, the exciplex relaxed in toluene directly to the ground state, without the formation of the CT state. The lifetime of the exciplex was 140 ps for the Zn dyads and 1–2 ns for the metal-free compounds in toluene.

## 1. Introduction

Since the initial discovery of C<sub>60</sub> or [60]fullerene and the development of a method for its preparation, the fullerenes have been used in the design of electron donor–acceptor (DA) molecular systems.<sup>1–12</sup> The fullerenes can function as electron acceptors or even as electron accumulators. As these molecules have a low absorbance at the visible wavelengths, an efficient donor–acceptor dyad containing a fullerene moiety should include a donor capable of picking up light quanta in the visible region.<sup>1,3,5</sup> A series of dyads, comprising a fully conjugated

porphyrin as a donor and a fullerene as an acceptor, have been synthesized and intensively studied.<sup>1,3,5</sup> It has been found that, in addition to the photoinduced charge transfer (CT), the primarily excited porphyrin donor can transfer its excitation energy to the fullerene acceptor. The combination of these two processes, the energy and electron transfer, determines the photochemical behavior of the dyad. The CT reaction is efficient in polar solvents such as benzonitrile, whereas in nonpolar media, the CT is unfavorable and the singlet excited state undergoes an intersystem crossing to the triplet state before its relaxation to the ground state.

Recently, a new series of DA compounds, the phytochlorin–C<sub>60</sub> dyads, have been synthesized and conformationally characterized.<sup>13</sup> The principal difference between these dyads and the porphyrin–C<sub>60</sub> dyads<sup>1,3,5</sup> is the utilization of a chlorophyll derivative, phytochlorin or its Zn complex, as the electron donor, instead of a fully conjugated porphyrin. The phytochlorin–C<sub>60</sub> dyads underwent desirable light-induced CT in benzonitrile. The processes preceding the CT state revealed, however, significant difference in the excitation energy relaxation pathways, compared to those reported for the porphyrin–fullerene dyads. In addition to the energy transfer from the primary excited phytochlorin to fullerene, we observed the formation of a transient state with new spectroscopic properties. This state was finally attributed to the phytochlorin–fullerene exciplex. In benzonitrile, the exciplex appeared to be a precursor of the CT state and altogether four transients were observed. In a nonpolar

<sup>†</sup> Tampere University of Technology.

<sup>‡</sup> University of Helsinki.

(1) Imahori, H.; Sakata, Y. *Adv. Mater.* **1997**, *9*, 537.

(2) Naito K.; Sakurai, M.; Egusa, S. *J. Phys. Chem. A* **1997**, *101*, 2350.

(3) Kuciauskas, D.; Lin, S.; Seely, G. R.; Moore, A. L.; Moore, T. A.; Gust, D.; Drovetskaya, T.; Reed, C. A.; Boyd, P. D. W. *J. Phys. Chem.* **1996**, *100*, 15926.

(4) Liddell, P. A.; Kuciauskas, D.; Sumida, J. P.; Nash, B.; Nguyen, D.; Moore, A. L.; Moore, T. A.; Gust, D. *J. Am. Chem. Soc.* **1997**, *119*, 1400.

(5) Imahori, H.; Hagiwara, K.; Aoki, M.; Akiyama, T.; Taniguchi, S.; Okada, T.; Shirakawa, M.; Sakata, Y. *J. Am. Chem. Soc.* **1996**, *118*, 11771.

(6) Sension, R. J.; Szarka, A. Z.; Smith, G. R.; Hochstrasser, R. M. *Chem. Phys. Lett.* **1991**, *185*, 179.

(7) Guldi, D. M.; Neta, P.; Asus, K.-D. *J. Phys. Chem.* **1994**, *98*, 4617.

(8) Maggini, M.; Scorrano, G.; Prato, M. *J. Am. Chem. Soc.* **1993**, *115*, 9798.

(9) Guldi, D. M.; Maggini, M.; Scorrano, G.; Prato, M. *J. Am. Chem. Soc.* **1997**, *119*, 974.

(10) Saricitfc, N. S.; Wudl, F.; Heeger, A. J.; Maggini, M.; Scorrano, G.; Prato, M.; Bourassa, J.; Ford, P. C. *Chem. Phys. Lett.* **1995**, *247*, 510.

(11) Nadochenko, V. A.; Denisov, N. N.; Rubtsov, I. V.; Lobach, A. S.; Moravskii, A. P. *Chem. Phys. Lett.* **1993**, *208*, 431.

(12) Nojiri, T.; Alam, M. M.; Konami, H.; Watanabe, A.; Ito, O. *J. Phys. Chem. A* **1997**, *101*, 7943.

(13) Helaja, J.; Tauber, A. Y.; Abel, Y.; Tkachenko, N. V.; Lemmetyinen, H.; Kilpeläinen, I.; Hynninen, P. H. *J. Chem. Soc., Perkin Trans. 1* **1999**, 2403.

solvent, e.g., toluene, the CT reaction was unfavorable and the exciplex relaxed directly to the ground state.

## 2. Experimental Section

**2.1. Compounds.** The reference compound, 3<sup>1</sup>,3<sup>2</sup>-didehydrophytochlorin methyl ester (**P<sub>ref</sub>**), and the phytochlorin-[60]fullerene dyads (**PF**, **PF<sub>Me</sub>**, and **ZnPF<sub>Me</sub>**) were prepared and conformationally characterized as described earlier.<sup>13</sup> The solvents used were of analytical grade, dried and stored over 4 Å molecular sieves.

**2.2. Steady-State Spectroscopy.** Absorption spectra were recorded on a Shimadzu UV-2501 PC spectrophotometer, with slits set to 1 nm. Steady-state fluorescence spectra were measured on a Fluorolog 3 spectrofluorimeter (ISA Inc.) equipped with a cooled IR-sensitive photomultiplier (R2658). The fluorescence spectra were corrected using the correction function supplied with the instrument. The excitation wavelength was at the maximum of the Soret band (410–430 nm region). The corrected emission spectra were recorded in the wavelength range from 600 to 1000 nm with the detection monochromator slits set to 2 nm and the accumulation time to 1 s.

**2.3. Time-Resolved Fluorescence Spectroscopy.** Fast fluorescence decays were measured by an up-conversion method.<sup>14</sup> The instrument comprised a Ti:sapphire femtosecond laser (TiF50, CDP-Avesta, Moscow, Russia) pumped by an Ar ion laser (Innova 316, Coherent). The radiation wavelength was centered at 820 nm, the pulse half-width was 50 fs, as estimated by using an autocorrelator, and the pulse repetition rate was 91 MHz. The instrument (FOG100, CDP-Avesta, Moscow, Russia) utilizes the second harmonic (410 nm) of the laser emission for the sample excitation. The fluorescence emitted from a rotating disk-shaped cuvette with an optical path length of 1.0 mm was collected by an achromatic lens with the focal distance of 40 mm. The fluorescence and the laser gate pulses (at 820 nm) were focused onto a 0.3 mm BBO nonlinear crystal (NLC), the sum frequency produced by it was selected by a monochromator, and its intensity was measured by a photomultiplier (R1527P, Hamamatsu) working in a photon counting regime. A typical time resolution of the system was 150 fs (fwhm). Fluorescence decay curves were fitted to a sum of exponents convoluted with an instrumental response function, measured in the same arrangement as the fluorescence but with the excitation pulse used instead of the emission pulse.

**2.4. Time-Resolved Absorption Spectroscopy.** Femtosecond to picosecond time-resolved absorption spectra were collected using a pump-probe technique. The femtosecond pulses of the Ti:sapphire generator were amplified by using a multipass amplifier (CDP-Avesta, Moscow, Russia) pumped by a second harmonic of the LF114 Nd:YAG Q-switched laser (Solar TII, Minsk, Belorussia). The amplified pulse energy varied from 0.3 to 0.5 mJ and the repetition rate was 10 Hz. The pulses were split into two beams. One beam (10%) was focused to a second harmonic generator (SHG) to produce excitation pulses (pump beam). Another beam was focused on a 4-mm sapphire plate to generate a white continuum (probe beam). The continuum was collimated by a lens and then split into two beams. The first beam was used for the transient absorption measurements and it crossed the sample on the same spot as the excitation beam. The second beam was used as a reference beam; it passed the sample across a nonexcited area. Finally the two beams were directed onto an input slit of a monochromator (Solar, Minsk, Belorussia) coupled with a cooled CCD detector (PI 1100 × 330, Princeton Instruments, USA). Each beam produced one stripe on the CCD image. The stripes were used to calculate intensity spectra for the signal,  $I_{\text{sig}}(\lambda)$ , and for the reference,  $I_{\text{ref}}(\lambda)$ , pulses. The wavelength range for a single measurement was 227 nm and typically two regions were studied, 550–780 and 820–1050 nm.

The ratio of the intensities,  $\alpha(\lambda) = I_{\text{sig}}(\lambda)/I_{\text{ref}}(\lambda)$ , was typically within 0.8–1.3. The ratio was recorded before the pump-probe experiments and was used for the correction of the measurement. Thus, during the pump-probe experiments the change in the optical density of the sample was calculated as  $\Delta\text{OD}(\lambda) = -\log\{[I_{\text{sig}}(\lambda)/I_{\text{ref}}(\lambda)]/\alpha(\lambda)\}$ . For a single measurement, the CCD shutter was open for 1 s and spectra of 10 pulses were averaged at once in the detector. Usually 10 measure-

ments were performed and averaged to improve the signal-to-noise ratio. Intensities and shapes of the reference spectra were checked and variations more than 10% were not accepted. This enabled one to achieve a resolution of 0.001–0.005 in the optical density (OD) units, depending on the wavelength. Time-resolved spectra were measured with a delay line moving in 100 fs steps for the first 2 ps period and then increasing the time step at longer delays. The increment factors were 1.1–1.3 to cover the whole time range of interest (100 fs – 1 ns) with 40–60 spectra.

To obtain quantitative information about the photochemical processes, the decay profiles were calculated out of the spectra with a wavelength averaging range of 3–5 nm. The decays were globally fitted to a sum of exponentials,

$$D(t, \lambda) = a_0(\lambda) + \sum a_i(\lambda) \exp(-t/\tau_i) \quad (1)$$

and deconvoluted with the Gaussian pulse

$$p(t) = \exp[-(t - s)^2/\tau_p^2] \quad (2)$$

where  $\tau_p$  is the pulse half-width and  $s = s(\lambda)$  is the probe pulse delay caused by the group velocity dispersion. The fit parameters were the lifetimes,  $\tau_i$ , the corresponding preexponential factors,  $a_i(\lambda)$ , pulse width,  $\tau_p$ , and the delay spectrum,  $s(\lambda)$ . The two last parameters were used mainly for evaluating the quality of the fit together with the mean-square deviation,  $\sigma^2$ . In test experiments, the pulse half-width was  $\tau_p \sim 60$ –90 fs, which corresponds to the time resolution of about 150 fs. The group velocity dispersion in the range of one spectrum, e.g., from 550 to 750 nm, was about 0.8 ps, thus an accurate determination of the delays,  $s(\lambda)$ , was important for the correct fitting of fast transients ( $t < 1$  ps). The probe pulse delay,  $s(\lambda)$ , can be fitted using two methods. First, the delay can be fitted independently at all wavelengths, which yields a delay spectrum. Second, the group velocity dispersion can be approximated by a polynomial of the second degree, which involves three global parameters to be fitted. The first method gave a better  $\sigma^2$ -value, but the spectra  $s(\lambda)$  were monotonic functions of wavelengths only in average and at some wavelengths deviations exceeded 0.5 ps, which reduced significantly the accuracy of the calculations for the short-lived component. The second method caused a small increase (2–3%) in the  $\sigma^2$ -value compared to the first method, but smoother component spectra were obtained for the shortest-lived component. Because the pulse width is a free parameter in the fitting procedure, it is impossible to distinguish the fast formation from the pulse broadening. This limits the resolution at lifetimes shorter than 300 fs. In that respect, the fluorescence up-conversion method gives a more accurate estimate for lifetimes shorter than 1 ps.

## 3. Results

**3.1. Structural Aspects.** The structures of the **PF**, **PF<sub>Me</sub>**, and **ZnPF<sub>Me</sub>** dyads are presented in Figure 1. The <sup>1</sup>H NMR spectra of the dyads revealed the presence of four different molecular species in the solutions.<sup>13</sup> These species represent a pair of diastereomers (epimeric at the 2'-position of the pyrrolidine ring) and a pair of atropisomers of each diastereomer, differing in the orientation of the fullerene ball regarding that of the propionic acid side chain of the phytochlorin ring (Figure 2). The atropisomerism is due to a rather short linkage between the C<sub>60</sub> ball and the chlorin ring, which restricts free rotation of the bulky ball. It was possible to separate chromatographically a mixture of the atropisomers into pure atropisomer  $\alpha$ -**PF** and atropisomer  $\beta$ -**PF** (Figure 2).

A comparative spectroscopic study of the two atropisomers was performed. Both the steady-state absorption and emission spectra were recorded for the  $\alpha$ - and  $\beta$ -**PF** compounds separately. Also the time-resolved fluorescence up-conversion and transient pump-and-probe methods were applied to each atropisomer separately. No differences were observed in any of the photochemical parameters determined. In addition, the pure  $\alpha$ -

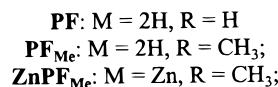
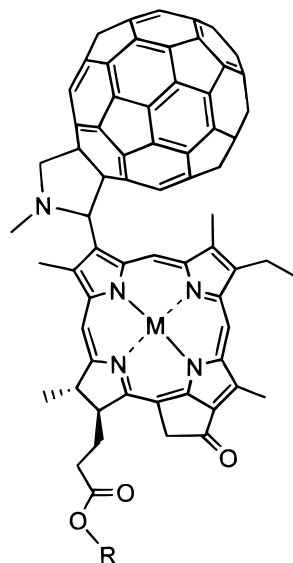


**Figure 1.** Structures of PF<sub>Me</sub>, PF, and ZnPF<sub>Me</sub> dyads.

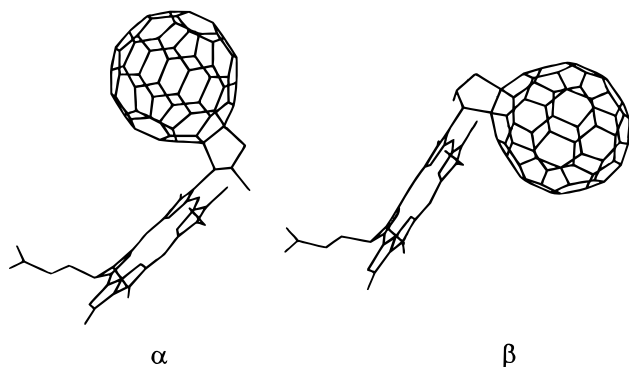


**Figure 2.** Atropisomers  $\alpha$ -PF and  $\beta$ -PF.

and  $\beta$ -atropisomers were separately subjected to a continuous irradiation with blue light (intensity was about 0.1 mW cm<sup>-2</sup> nm<sup>-1</sup> at 410 nm) for a period of 1 h, but no photoisomerization was observed in either case. Thus, the photochemistry is the same for both atropisomers within experimental errors, and there is no need to distinguish the atropisomers from each other in the photochemical characterizations of the three forms of the DA dyads (PF, PF<sub>Me</sub>, and ZnPF<sub>Me</sub>). Only minor differences (mainly in the rates of individual reaction steps) were observed in the photochemical behavior of the carboxylic acid dyad (PF) as compared to that of the methylated dyad (PF<sub>Me</sub>).

**3.2. Steady-State Spectroscopy.** The steady-state absorption spectra of 3<sup>1</sup>,3<sup>2</sup>-didehydropyrylochlorin methyl ester (P<sub>ref</sub>), methylated phytychlorin–fullerene (PF<sub>Me</sub>), and [60]fullerene in toluene are shown in Figure 3. To a great extent the absorption spectrum of PF<sub>Me</sub> is a superposition of the spectra of P<sub>ref</sub> and C<sub>60</sub>. Small perturbations in the spectrum of the PF<sub>Me</sub> dyad indicate a weak electronic interaction between the phytychlorin and the fullerene chromophores in the ground state.

In the time-resolved experiments, the absorption of the phytychlorin part at the excitation wavelength (400–420 nm) was much greater than that of the fullerene part. Therefore, mainly the phytychlorin moiety, i.e., the donor, was excited when the fluorescence up-conversion and transient absorption pump–probe methods were applied.

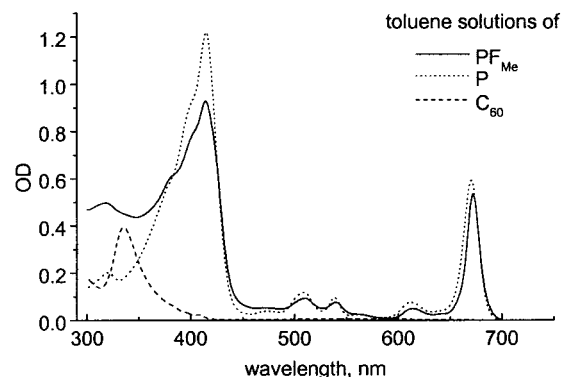
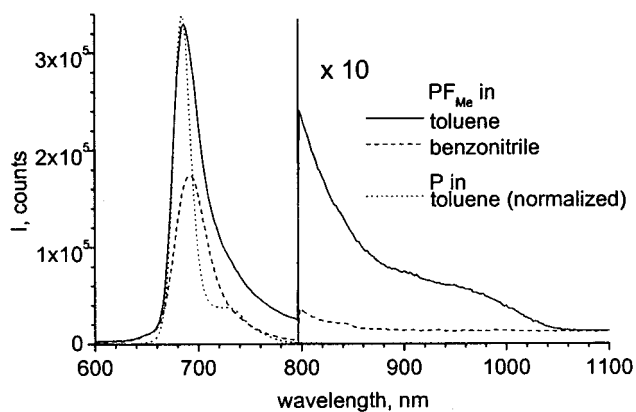


**Figure 3.** Absorption spectra of PF<sub>Me</sub> (solid line), P (dotted line), and C<sub>60</sub> fullerene (dashed line) in toluene; concentrations 12  $\mu$ M (1 cm cuvette).

a)



b)

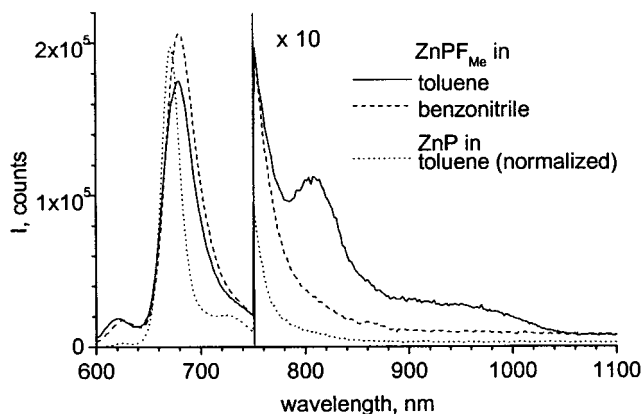


**Figure 4.** Corrected steady-state fluorescence spectra at visible and NIR wavelength ranges for (a) PF<sub>Me</sub> and (b) ZnPF<sub>Me</sub> in toluene (solid line) and benzonitrile (dashed line). The normalized fluorescence spectra of the corresponding reference compounds (P and ZnP) are shown by dotted lines.

The intensities of the steady-state fluorescence of the DA compounds, originating mainly from the phytychlorin moiety, were quenched to a value of 1/200 relative to the intensity of the pure reference molecule, P<sub>ref</sub>. The efficiencies of the quenching were almost the same for the three DA dyads in all solvents. The fluorescence spectra of P<sub>ref</sub>, PF<sub>Me</sub>, and ZnPF<sub>Me</sub> are shown in Figure 4. In the Q-band region, at about 680 nm, a small red shift (1.5–2 nm for the metal-free dyads and 8 nm for the Zn dyad) and a broadening of the fluorescence bands



can be seen for the DA dyads compared to the bands of the reference compounds,  $P_{\text{ref}}$  and  $ZnP_{\text{ref}}$ . At longer wavelengths, a broad shoulder in the fluorescence spectra of  $PF_{\text{Me}}$  and  $ZnP_{\text{Me}}$  can be seen, being most pronounced in toluene. In the case of the toluene solution of  $ZnP_{\text{Me}}$ , even a formation of a new emission band at 810 nm was observed. The band was not observed for the free-base derivatives ( $PF$  and  $PF_{\text{Me}}$ ), thus it cannot be attributed to the fluorescence of the fullerene part alone. To our knowledge, this is the first indication of an observable emissive transient and of the possible difference between the reaction mechanisms in polar and nonpolar solvents.

**3.3. Time-Resolved Fluorescence Decays.** The time-resolved fluorescence measurements of the studied compounds were carried out by the fluorescence up-conversion technique. The decays were followed at the 670–680 nm wavelengths, which are around the  $\lambda_{\text{max}}$  of the steady-state fluorescence of the phytochlorin moiety, at 710 nm, which is in the range of the fullerene fluorescence,<sup>1,15–17</sup> and at 750 nm, which is the red-wavelength limit of the instrument. The decays were measured with a 25 fs delay step to resolve the short-lived components and with 0.1–2 ps steps to detect the long-lived components. The decays were fitted separately to two and three exponentials, and only fittings with weighted mean-square deviation,  $\chi^2$ , better than 1.1 were considered as successful. The relative intensities of the short-lived components at 670 nm were higher than 60% for  $PF_{\text{Me}}$  and  $PF$  in toluene and higher than 90% in benzonitrile and  $ZnP_{\text{Me}}$  in all solvents. In all cases, the lifetimes of the short-lived components were 200–250 fs for  $ZnP_{\text{Me}}$  and 300–900 fs for  $PF_{\text{Me}}$  and  $PF$ . The long-lived component was detected at 680 nm, and it became more pronounced at longer wavelengths.

The fluorescence decays of  $PF_{\text{Me}}$  and  $ZnP_{\text{Me}}$  in benzonitrile are shown in Figures 5 and 6, respectively. The fast component of  $PF_{\text{Me}}$  had a lifetime of ca. 0.5 ps and it was dominant at wavelengths 675 and 710 nm (Figure 5a,b), where also a component with a lifetime of about 3 ps was observed. Another long-lived component was observed at 750 nm (Figure 5c). Its lifetime was approximately 10 ps, but its intensity was relatively low and hence an accurate lifetime determination was not possible. The remaining fluorescence had a lifetime in the nanosecond time domain and it was measured using the time-correlated single photon counting technique. Most probably this remaining fluorescence originated from a small amount of impurities or self-aggregates present in the sample. A photochemical behavior, similar to that of  $PF_{\text{Me}}$ , was observed for  $ZnP_{\text{Me}}$  in benzonitrile (Figure 6). The corresponding lifetimes were 220 fs, 1.9 ps, and 6.1 ps.

Unfortunately, a photodegradation of the studied compounds was observed in toluene during the up-conversion measurements. This did not allow us to resolve the long-lived components, as the measurements at longer wavelengths needed longer accumulation times. The short-lived component was dominant in the fluorescence decays in the wavelength range of 670–680 nm, with lifetimes of ca. 900 fs for  $PF_{\text{Me}}$ , 600 fs for  $PF$ , and 230 fs for  $ZnP_{\text{Me}}$ , respectively.

**3.4. Transient Absorption Studies.** The transient absorption measurements were carried out in two wavelength domains: around the Q-band (550–780 nm) and in the NIR region (820–1050 nm). The visible region was important for following the

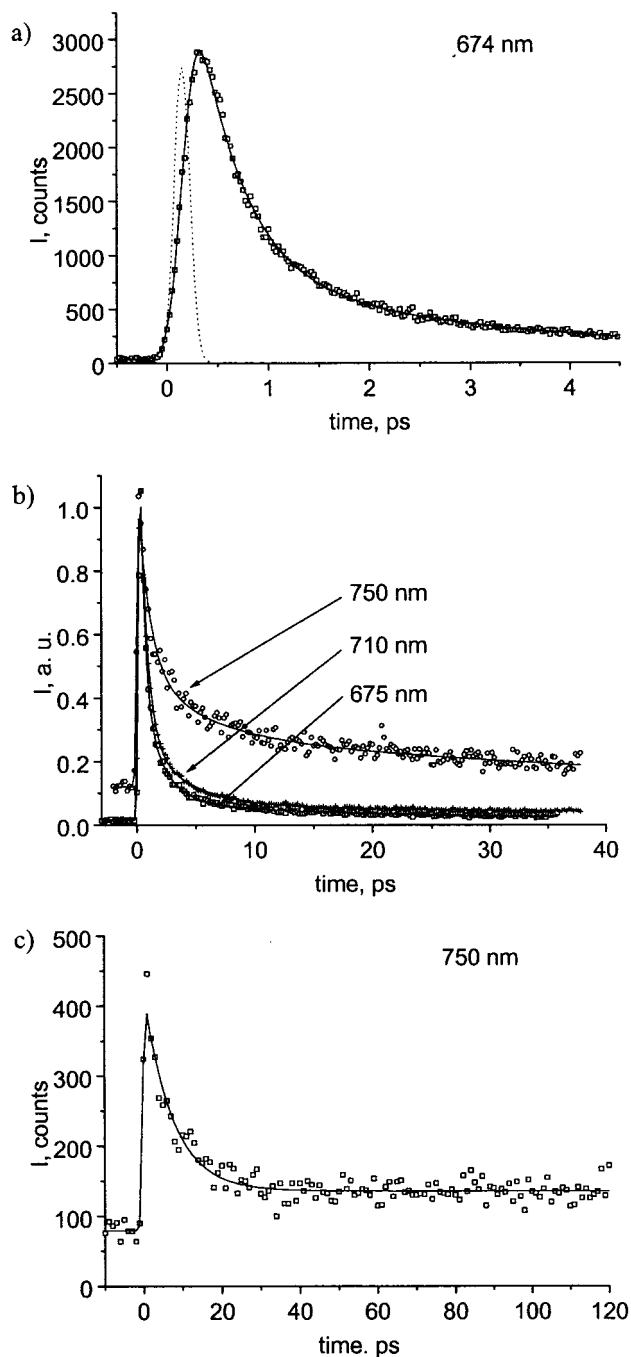


**Figure 5.** Fluorescence decay curves of  $PF_{\text{Me}}$  in benzonitrile in different time scales at (a) 674 nm (dotted line is the instrument response function), (b) 675, 710, and 750 nm, and (c) 750 nm. The fitted curves are shown as solid lines.

photoinduced perturbations occurring in the phytochlorin part, whereas the NIR region gave information about the photochemistry of the fullerene part of the dyads.

**3.4.1. Transient Absorption at the Q-Band of the Dyads in Toluene.** When the transient absorption data obtained in toluene were globally fitted, an approximation with three exponentials gave a reasonable mean-square deviation,  $\sigma^2$ , for all three DA dyads. The addition of the fourth exponential to the fitting did not improve the statistical reliability in terms of the mean-square deviation (the typical decrease in the  $\sigma^2$ -value was 2–5%), and a fitting with two exponentials caused statistically worse results (the  $\sigma^2$ -value was 1.5–2 times as high as that for the fitting with three exponentials).

(15) Sun, Y.-P.; Wang, P.; Hamilton, N. B. *J. Am. Chem. Soc.* **1993**, *115*, 6378.

(16) Guldi, D. M.; Torres-Garcia, G.; Mattay, J. *J. Phys. Chem. A* **1998**, *102*, 9679.

(17) Sun, Y.-P.; Lawson, G. E.; Riggs, J. E.; Ma, B.; Wang, N.; Moton, D. K. *J. Phys. Chem. A* **1998**, *102*, 5520.

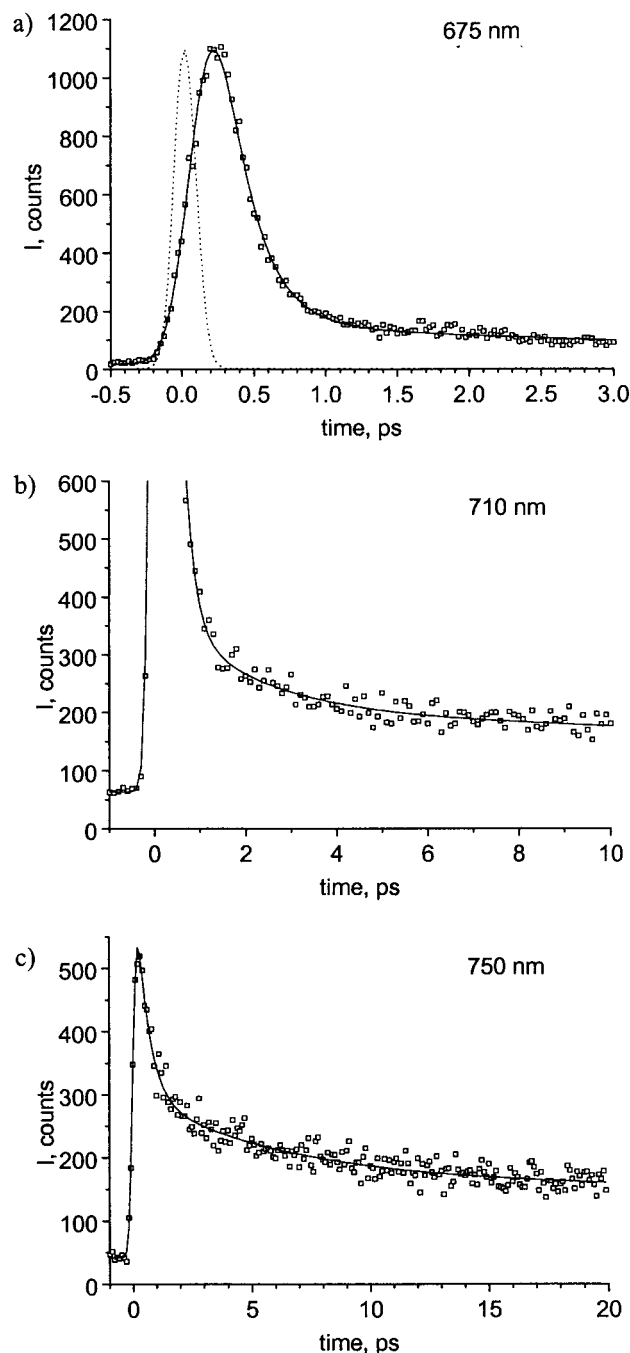


**Figure 6.** Fluorescence decay curves of **ZnPF<sub>Me</sub>** in benzonitrile in different time scales at (a) 680 nm,  $\tau = 210$  fs (94%) (dotted line is the instrument response function), (b) 710 nm,  $\tau_1 = 220$  fs (93%) and  $\tau_2 = 1.9$  ps (4%) (the vertical scale is magnified to demonstrate the 1.9 ps component), and (c) 750 nm,  $\tau_1 = 0.52$  ps (61%) and  $\tau_2 = 6.1$  ps (21%). The fitted curves are shown as solid lines.

The component spectra for **PF** and **ZnPF<sub>Me</sub>**, at the Q-band region, obtained by fitting with three exponentials, are shown in Figure 7. Three components for both compounds can be observed at  $\sim 670$  nm. The time-resolved transient signals measured at selected wavelengths for **PF** are shown in Figure 8. The signal at 673 nm was formed in 200–300 fs (Figure 8a) and was characterized by a strong bleaching of the Q-band. Tentatively this state was attributed to the first excited singlet state of the phytychlorin chromophore. The fast bleaching is followed by a 30–40% recovery with a time constant of 0.6 ps (Figure 8a). This rate correlates well with the short-lived component in the fluorescence decay. The recovery process is

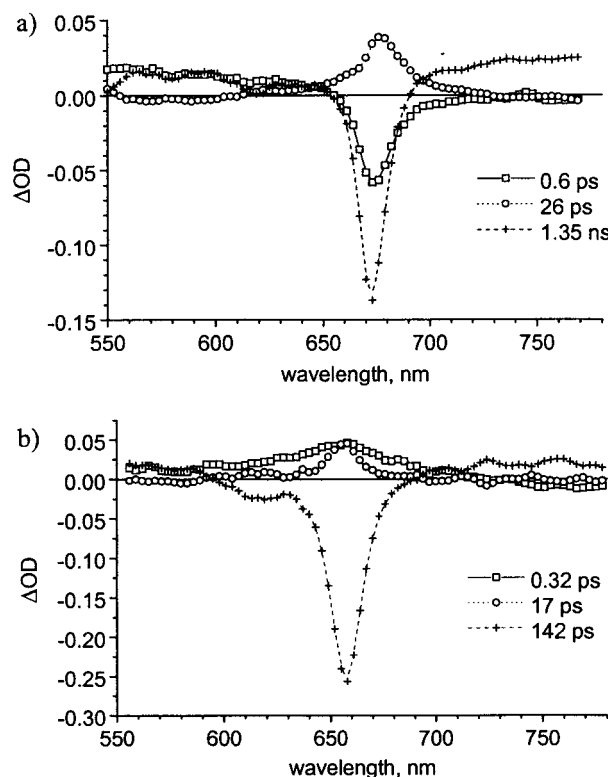


**Figure 7.** Transient absorption decay component spectra of (a) **PF** and (b) **ZnPF<sub>Me</sub>** in toluene. Lifetimes of the components are indicated.

followed by a decrease in the optical density with the lifetime of 26 ps and an increase in the density with the lifetime of 1.3 ns (Figure 8b). This process finally led to the ground state.

An important feature of the long-lived component, with the lifetime of 1.35 ns for **PF**, is the broad absorption band at the 750 nm region. This band is formed extremely fast, as illustrated in Figure 8c. From the 685 nm decay curve one can estimate the relaxation of the singlet excited state with the time constant of 0.6–0.9 ps. This is consistent with the lifetime of the singlet state obtained using the time-resolved fluorescence up-conversion method. The singlet state relaxation was clearly slower than the formation of the absorption at 748 nm. The latter occurs in 200–300 fs, which is at the limit of the time resolution of our instrument.

**3.4.2. Transient Absorption at the Q-Band of the Dyads in Benzonitrile.** Transient component spectra of the DA compounds, measured in benzonitrile, were more complex than those measured in toluene. In benzonitrile, a fitting with four exponentials was necessary to obtain an acceptable value for the mean-square deviation,  $\sigma^2$ . The component spectra of **PF** are presented in Figure 9. Consistent with the results obtained for the toluene solutions, the photoexcitation in benzonitrile resulted in a bleaching of the ground-state absorption at the Q-band region, but at the later stage, the spectra exhibited a red shift for the Q-band. Comparison of the component spectra obtained in benzonitrile for **PF** with those observed in toluene (Figure 7a) reveals that the similar three components are also present in benzonitrile solutions. The fourth component, which does not appear in toluene, has the longest lifetime of 70 ps for **PF**. Its spectrum corresponds to a shift rather than bleaching of the Q-band.

Another important observation is that the transient absorption band at 748 nm relaxes faster than the 70 ps component (Figure 9b). Formation of the absorption at 682 nm takes place with the time constant similar to the lifetime of the transient signal

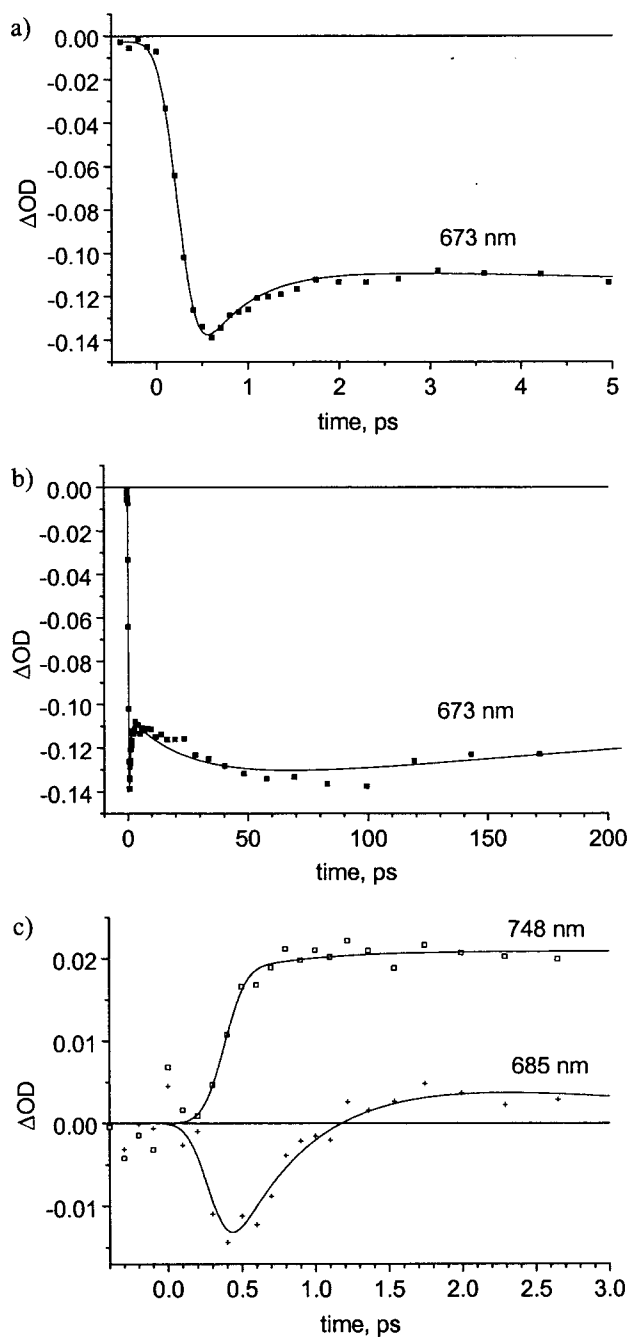


**Figure 8.** Time-resolved transient absorption curves of **PF** in toluene at different wavelengths. For details see the text. The solid lines correspond to the global fittings with the lifetimes indicated in Figure 7.

at 748 nm. The longest-lived signals were observed mainly at the Q-band region. The signals correspond to the increase in optical density at the red shoulder (682 nm) and to the decrease at the blue shoulder (661 nm). A similar behavior was observed for **ZnPF<sub>Me</sub>** in benzonitrile. Its component spectra are shown in Figure 10. A fitting with four exponentials was needed to achieve a reasonable  $\sigma^2$ -value. The new longest-lived component has spectroscopic features similar to those of the longest-lived component observed for **PF** in benzonitrile.

**3.4.3. Transient Absorption of the Dyads at NIR Wavelengths.** The transient species of all DA compounds at the NIR wavelengths (820–1050 nm) were formed fast (<1 ps) in both toluene and benzonitrile. In toluene, the absorption relaxed with a lifetime close to that observed for the longest-lived component

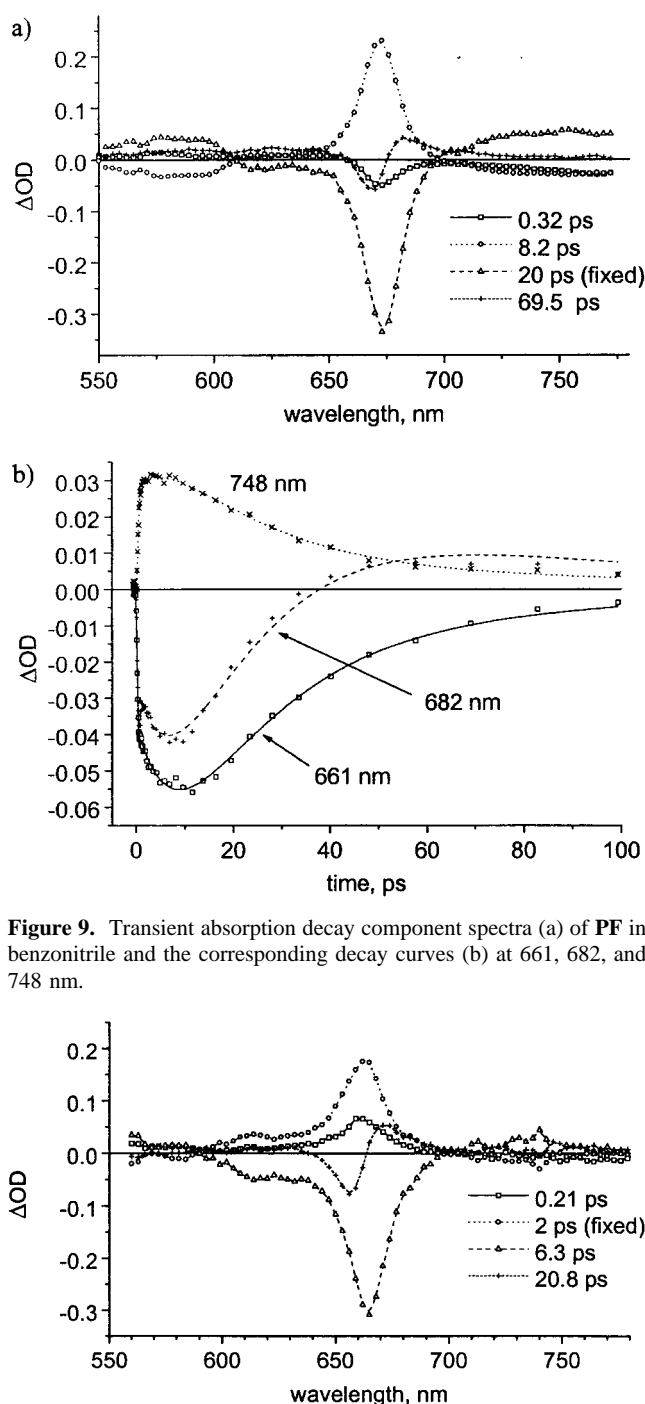


**Figure 9.** Transient absorption decay component spectra (a) of **PF** in benzonitrile and the corresponding decay curves (b) at 661, 682, and 748 nm.

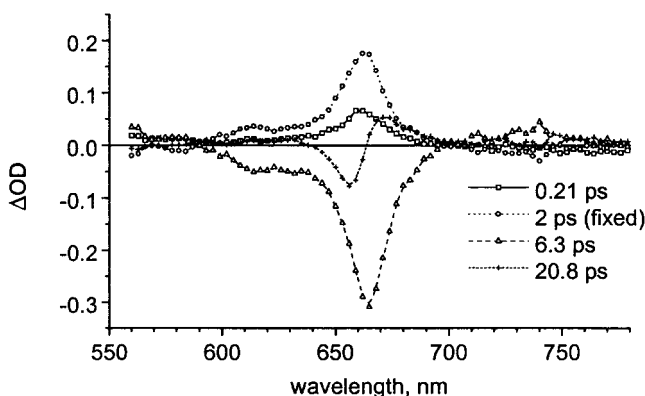


**Figure 10.** Transient absorption decay component spectra of **ZnPF<sub>Me</sub>** in benzonitrile. The corresponding lifetimes are indicated.

at the Q-band region, e.g., ca. 1 ns for **PF** and **PF<sub>Me</sub>** and ca. 150 ps for **ZnPF<sub>Me</sub>**.

In benzonitrile, the lifetimes of the transients at the NIR region were about 20 ps at 850 nm and about 70 ps at 1000 nm for **PF**. The measured transient spectra at selected delays are shown in Figure 11b, where clear differences in decays at 850 and 1000 nm regions can be seen.

#### 4. Discussion

The excitation of the studied dyads took place at about 400 nm resulting in the formation of the second excited singlet state of the phytochlorin donor,  $^3P_{S_2}F$ , since the extinction coefficient of the phytochlorin part at this wavelength is much higher than

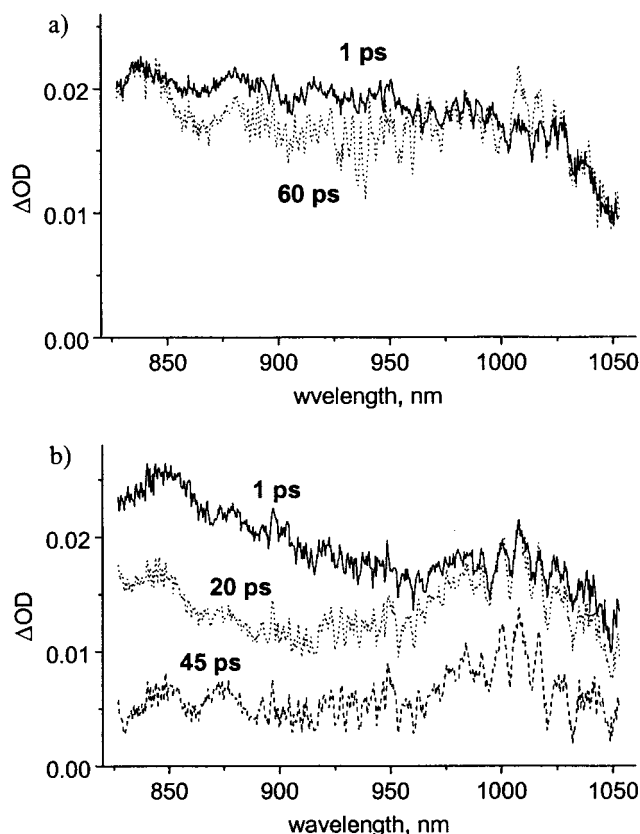


**Figure 11.** Transient absorption spectra in the NIR region for **PF** in (a) toluene and (b) benzonitrile. Delay times are indicated in the figure.

that of the fullerene part. Usually, the second excited state relaxes fast to the first excited state. The energy levels of the first singlet excited states of the phytychlorin and fullerene moieties are quite close to each other (1.86 eV for **ZnP**, 1.83 eV for **P<sub>ref</sub>**, and 1.74 eV for [60]fullerene<sup>3</sup>), and the distance between the covalently linked chromophores is rather short, 8–10 Å center-to-center. Thus, one can expect an efficient and reversible energy transfer from the phytychlorin moiety to the fullerene ball. A comparable energy transfer was observed previously to occur in the porphyrin–fullerene dyads.<sup>3</sup> Therefore, the singlet excited state of the fullerene, **P<sup>\*</sup>F<sub>S1</sub>**, can be formed. Since the molecules are composed of donor and acceptor, the formation of a charge transfer (CT) state, **P<sup>+</sup>F<sup>-</sup>**, can be expected. If the CT state is energetically unfavorable, one can expect an appearance of a triplet excited state, **P<sup>\*</sup>T<sub>F</sub>** or **P<sup>\*</sup>F<sub>T</sub>**. Thus, altogether six intermediate states are possible: **\*P<sub>S2</sub>F**, **\*P<sub>S1</sub>F**, **P<sup>\*</sup>F<sub>S1</sub>**, **P<sup>+</sup>F<sup>-</sup>**, **\*P<sub>T</sub>F**, and **P<sup>\*</sup>F<sub>T</sub>**. By analyzing the fluorescence and transient absorption data, one can distinguish between the possible reaction pathways and intermediate states.

The transient absorbances at the NIR region are mainly determined by the photoproducts of the fullerene moiety,<sup>18–23</sup> whereas the transient absorbances at the visible part of the spectrum are mainly induced by photoproducts of the phy-

tychlorin moiety. In particular, the bleaching of the Q-band absorption indicates that the electron sub-system of the phytychlorin is not in the ground state. An important qualitative observation is that, at long delay times (>10 ps), transient absorption signals decay almost simultaneously at the Q-band and at the NIR regions. Therefore, one can rule out the existence of triplet states, in which the triplet excitation is localized either on the phytychlorin or the fullerene moiety. The second reason to exclude the formation of triplet states is the short lifetime (<2 ns) of the transients.

It is known that the fullerene anion has an absorption band at 1000 nm.<sup>20–23</sup> Thus, the longest-lived transient observed at this wavelength in benzonitrile (for both Zn and metal-free DA dyads) can be attributed to a CT state, **P<sup>+</sup>F<sup>-</sup>** (Figure 11). The spectrum of the longest-lived component in the shorter wavelength range (Figure 9a) with the lifetime of 70 ps represents the differential spectrum between the CT state and the ground state. If the quantum yield of the CT state is known, its spectrum can be calculated.

It is noticeable, that the CT state was not observed in toluene for either of the DA dyads. Similar behavior was observed for the porphyrin–fullerene dyads,<sup>3</sup> in which the CT state was formed in benzonitrile, but did not appear in toluene either for the Zn or for the metal-free porphyrin derivatives. The CT state was observed, however, for the Zn porphyrin–fullerene dyad in benzene by Sakata et al.<sup>5</sup> For the **PF** compounds the main difference between the photochemical behavior of the dyads in toluene and in polar solvents was the existence of the fourth component, i.e., the CT state, in polar solvents. The lifetimes of the transient species varied from solvent to solvent, but their spectra were essentially similar.

To analyze the photochemical pathways of the dyads in toluene and in benzonitrile, one has to consider three intermediate states in the time domain from 200 fs (the ultimate time resolution of the particular measurements) to hundreds of picoseconds.

Eventually, the relaxation from the second singlet excited state, **\*P<sub>S2</sub>F**, to the first singlet excited state, **\*P<sub>S1</sub>F**, occurs faster than in 200 fs, since the fluorescence signal was formed in a time shorter than 200 fs. The strongest transient absorption signal was observed at the Q-band region. This signal is mainly due to the bleaching of the ground-state absorbance and its formation is determined by the instrumental time resolution. This time was 200–300 fs, depending on the solvent and the wavelength.

The shortest-lived component in all experiments had a lifetime shorter than 1 ps. The results from the fluorescence measurements implied that this component corresponds to the relaxation of the first singlet excited state, **\*P<sub>S1</sub>F**. It can be seen at the Q-band region as the recovery of the ground-state absorption (Figure 7a, the 0.6 ps component, and Figure 8a). The mechanism of the **\*P<sub>S1</sub>F** quenching is an energy transfer to the fullerene moiety, **P<sup>\*</sup>F<sub>S1</sub>**. The same phenomenon was also reported for the porphyrin–fullerene dyads.<sup>3</sup> This process was well resolved in time for **PF<sub>Me</sub>** and **PF** in toluene. It is noteworthy that about 60% of the initial bleaching remained when the energy transfer was complete (Figure 8a). Thus, part of the excited molecules did not proceed via an energy-transfer step, or did not appear originally in the **\*P<sub>S1</sub>F** state.

The following state, both in toluene and in benzonitrile, was that which dominated in the transient absorption in the time range of tens of picoseconds (Figures 7–10). This transient is characterized by a strong bleaching of the ground-state absorption of the phytychlorin chromophore at the visible part of the spectrum and by a broad ill-structured absorption at the NIR

(18) Ebbesen, T. W.; Tanigaki, K.; Kuroshima, S. *Chem. Phys. Lett.* **1991**, *181*, 501.

(19) Palit, D. K.; Sapre, A. V.; Mittal, J. P.; Rao, C. N. R. *Chem. Phys. Lett.* **1992**, *195*, 1.

(20) Kato, T.; Kodama, T.; Shida, T.; Nakagawa, T.; Matsui, Y.; Suzuki, S.; Shiromaru, H.; Yamauchi, K.; Achiba, Y. *Chem. Phys. Lett.* **1991**, *180*, 446.

(21) Greaney, M. A.; Gorum, S. M. *J. Phys. Chem.* **1991**, *95*, 7142.

(22) Fukuzumi, S.; Nakanishi, I.; Maruta, J.; Yorisue, T.; Suenobu, T.; Itoh, S.; Arakawa, R.; Kadish, K. M. *J. Am. Chem. Soc.* **1998**, *120*, 6673.

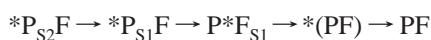
(23) Sun, Y.; Drovetskaya, T.; Bolskar, R. D.; Bau, R.; Boyd, P. D. W.; Reed, C. A. *J. Org. Chem.* **1997**, *62*, 3642.



range. Thus, both chromophores contribute to that state. On the other hand, the state is not the CT state, as can be seen from the spectra at both the NIR and visible wavelengths. Since the corresponding lifetime can be found in the fluorescence decays at the NIR wavelengths (Figures 5c and 6c), this state corresponds to an electronically excited state. In polar solvent, the relaxation of this state resulted in the formation of the CT state, and hence the state is a precursor of the CT state. The behavior of this state resembles the behavior of an exciplex. The energy of the exciplex must be lower than that of either the phytochlorin or the fullerene chromophore. Therefore, in the fluorescence spectrum, the exciplex may manifest itself at the NIR range, 800–1000 nm, which agrees well with the observed spectra (Figure 4).

The state described above is referred to as an intramolecular exciplex,  $^*(PF)$ . An obvious formation pathway of the exciplex is  $P^*F_{S1} \rightarrow ^*(PF)$ , which can be seen as a growth of the transient absorption signal recorded at 673 nm (Figure 8b). This transition is not observable at the NIR region as the spectra of  $P^*F_{S1}$  and  $^*(PF)$  states are similar. For **PF** in toluene, the formation of  $^*(PF)$  takes place in 26 ps. If the  $^*(PF)$  state does not absorb at the Q-band region, the excitation efficiency can be estimated to be about 50% under the experimental conditions used in this study.

If the pathway



would be the only road to reach the  $^*(PF)$  state, a complete recovery of the absorbance at the Q-band would be expected when the  $P^*F_{S1}$  state is reached. That clearly was not the case. The energy transfer from the excited phytochlorin moiety to the fullerene part is a fast and reversible process. Therefore, it may result in incomplete recovery of the Q-band bleaching in the reaction:



In the present case, the reaction balance is shifted more to the direction of  $P^*F_{S1}$ . This can be seen from the time-resolved fluorescence decay curves (Figures 5 and 6); the fast decay components dominate for all dyads in all solvents.

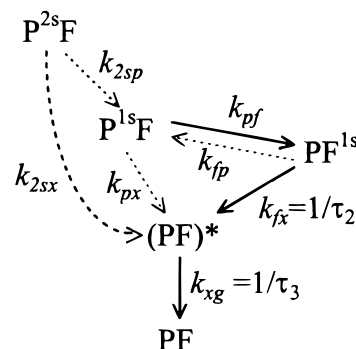
In addition to the formation of the exciplex from the  $P^*F_{S1}$  state, it may be formed also from the first excited singlet state of the phytochlorin moiety,  $^*P_{S1}F \rightarrow ^*(PF)$ . This was, however, not observed experimentally. The exciplex has a broad absorption band at 750 nm (Figure 7) that is formed faster than the  $^*P_{S1}F$  state decayed, as illustrated in Figure 8c by the transient absorption curve at 748 nm. Therefore the  $^*(PF)$  state is, at least partially, formed before the  $^*P_{S1}F$  state is totally relaxed. Thus, the possibility that  $^*(PF)$  is formed directly from the second singlet excited state,  $^*P_{S2}F$ , should be taken into account:  $^*P_{S2}F \rightarrow ^*(PF)$ .

In toluene the transient absorption signal decays simultaneously at all wavelengths, thus the exciplex relaxes directly to the ground state. Probably the energy of the exciplex in toluene is somewhat lower than the energies of the triplet states of either the phytochlorin or the fullerene.

Finally, a kinetic scheme for the photoinduced processes in toluene is presented in Scheme 1, where solid arrows represent processes resolved experimentally and dotted arrows describe processes which are either too fast to be measured directly or are inefficient to be detected reliably.

As shown in Scheme 1, two processes can be associated with the experimentally detected lifetimes. In the case of **PF** in

Scheme 1



toluene solution these are  $\tau_2 = 26$  ps =  $1/k_{fx}$ , which represents the  $P^*F_{S1} \rightarrow ^*(PF)$  transition, and  $\tau_3 = 1.3$  ns =  $1/k_{xg}$ , which is the lifetime of the  $^*(PF)$  state. The shortest lifetime,  $\tau_1 = 0.6$  ps, is associated with the relaxation of the first singlet excited state,  $^*P_{S1}F$ . The reaction  $^*P_{S1}F \rightarrow ^*(PF)$  is possible, but was not observed in the transient absorption decay curves and, thus, seems not to be efficient. Therefore, one can conclude that  $k_{pf} \gg k_{px}$  and  $\tau_1 \approx 1/k_{pf}$ . The dominating reaction in the energy transfer is  $^*P_{S1}F \rightarrow P^*F_{S1}$ , but the reverse reaction,  $P^*F_{S1} \rightarrow ^*P_{S1}F$ , is also possible since the fluorescence spectrum of the fullerene somewhat overlaps the absorption spectrum of the phytochlorin moiety. This would result in a biexponential decay of the phytochlorin fluorescence, which was observed experimentally. However, the second component in the fluorescence decay at 675 nm was relatively small, e.g. less than 10% for the benzonitrile solutions, which means that the forward energy transfer is more efficient than the reverse one.

The relaxation rate of the  $^*P_{S2}F$  state is given by the sum of two rate constants,  $k_{2sp} + k_{2sx}$ , and could, in principle, be observed, but is too fast to be resolved experimentally. A hint for the fast formation of the  $^*(PF)$  state is seen in Figure 8c. The formation of the transient at 748 nm takes place in a time of about 0.1 ps, which corresponds to the ultimate time resolution of the instrument.

According to Scheme 1, all the excited molecules converted into the  $^*(PF)$  state before the relaxation to the ground state. In the case of **PF<sub>Me</sub>** and **PF**, the lifetime of the  $^*(PF)$  state is much longer than lifetimes of its precursors. Thus the spectrum of the longest-lived component,  $a_3(\lambda)$ , can be obtained as a difference between the spectrum of the  $^*(PF)$  state and that of the ground state, **PF**:

$$a_3(\lambda) = [S_x(\lambda) - S_{gr}(\lambda)]\phi \quad (3)$$

where  $S_{gr}(\lambda)$  is the ground-state spectrum,  $S_x(\lambda)$  is the spectrum of the exciplex, and  $\phi$  is the relative amount of excited molecules.

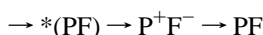
The  $^*(PF)$  state is characterized by a strong bleaching of the Q-band and the energy of this state should be lower than that of the Q-band. Therefore it is reasonable to suggest that the exciplex does not absorb at the Q-band region. In the case of **PF** in toluene, a flat absorption spectrum at the Q-band region can be achieved when  $\phi = 0.45$ . The resulting spectrum,  $S_x(\lambda) = S_{gr}(\lambda) + a_3(\lambda)/\phi$ , is shown in Figure 12 (solid line). The intensities of the spectra of the  $^*P_{S1}F$  and  $P^*F_{S1}$  states ( $S_p(\lambda)$  and  $S_f(\lambda)$ , respectively) depend on the relative fractions of the species in the reaction path  $^*P_{S2}F \rightarrow ^*P_{S1}F \rightarrow P^*F_{S1}$  compared to those in the path  $^*P_{S2}F \rightarrow ^*(PF)$ . If the relative fraction of the molecules relaxing via the  $^*P_{S1}F$  state is  $\beta$ , then one can write:

$$a_2(\lambda) = [S_f(\lambda) - S_x(\lambda)]\phi\beta \quad (4)$$

$$a_1(\lambda) = [S_p(\lambda) - S_f(\lambda)]\phi\beta \quad (5)$$

where  $S_p(\lambda)$  and  $S_f(\lambda)$  are spectra of the  $^*P_{S1}F$  and  $P^*F_{S1}$  states, respectively. At the Q-band maximum, the absorption of the  $P^*F_{S1}$  state should be approximately equal to that of the ground state (since the phytychlorin chromophore is in the ground state), whereas at the  $^*P_{S1}F$  state the Q-band should be essentially bleached. Thus, the  $\beta$  fraction can be estimated as  $\beta \approx -a_2/a_3$  or  $\beta \approx a_1/a_3$  at the wavelength of about 670 nm. A reasonable estimate for  $\beta$ -values would be in the range of 0.3–0.4. An average value of 0.35 has been used to calculate the spectrum of  $P^*F_{S1}$ , presented in Figure 12.

In benzonitrile, four transient species were observed. Thus, the CT state should be added to Scheme 1. It has the longest lifetime (70 ps) and is formed and relaxed by processes



Consequently, the spectrum of the longest-lived component,  $a_4(\lambda)$ , can be obtained as a difference between the spectrum of the CT state and that of the ground state, PF:

$$a_4(\lambda) = [S_{ct}(\lambda) - S_{gr}(\lambda)]\phi \quad (6)$$

where  $S_{ct}(\lambda)$  is the spectrum of the CT state. The spectrum of the exciplex in benzonitrile is given by

$$a_3(\lambda) = [S_x(\lambda) - S_{ct}(\lambda)]\phi \quad (7)$$

Following the procedure described for the toluene solution, one can determine the  $\phi$ -values and calculate the spectra for the  $^*(PF)$  and  $P^+F^-$  states. Results are presented in Figure 13. As can be seen, the intensity of the fullerene anion absorption at the wavelength range of about 1000 nm is surprisingly low, compared to the intensities of the fullerene excited state and the exciplex. Therefore, one can suggest that not all molecules of the  $^*(PF)$  state relax via the CT state, and that the quantum yield of the CT state formation is below unity. If the case of competitive relaxation of the exciplex via CT or directly to the ground state will be considered, then the calculated spectrum of the CT state would be characterized by greater absorbance of the fullerene anion. At the same time, a gradual decrease in the intensity and an increase in the red shift of the chlorin Q-band would be observed as a consequence of the formation of the chlorin  $\pi$ -cation radical.

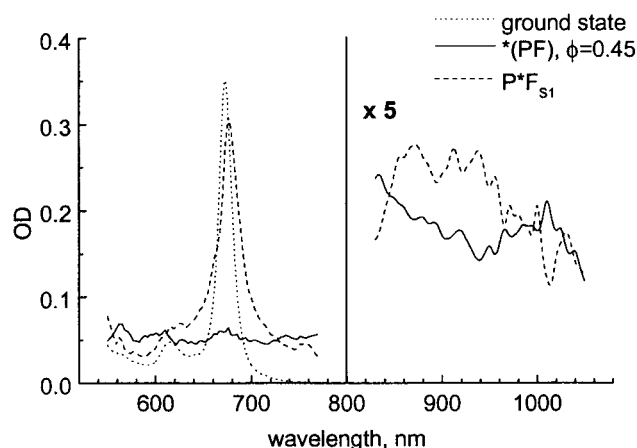


**Figure 12.** Transient absorption spectra of the  $^*(PF)$  (solid line) and  $P^*F$  (dashed line) states calculated for **PF** in toluene according to Scheme 1. The ground-state absorption is shown as the dotted line.

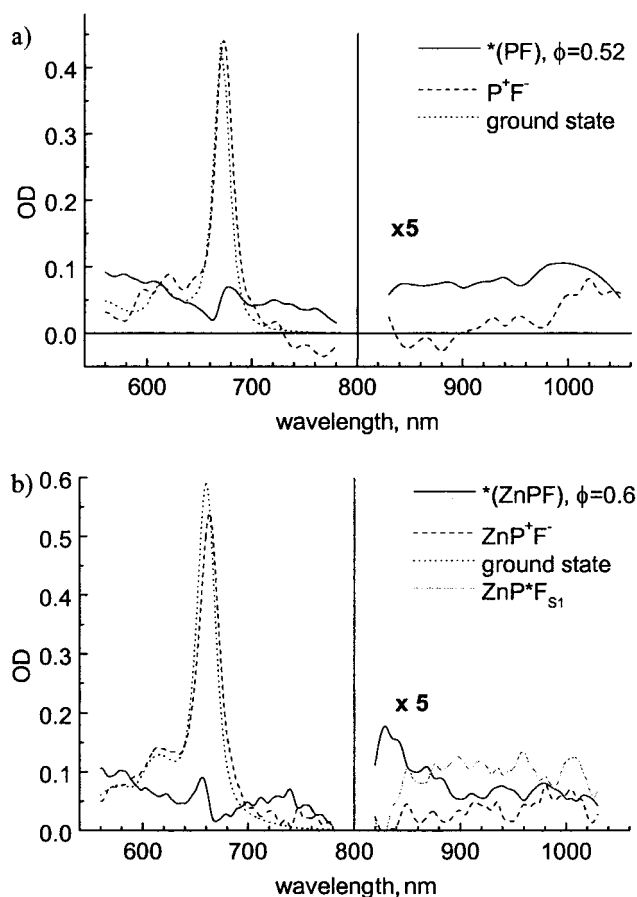
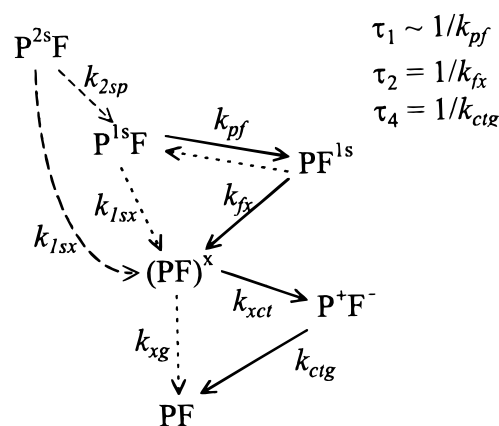


**Figure 13.** Transient absorption spectra of the  $^*(PF)$  (solid line) and CT (dashed line) states for (a) **PF**<sub>Me</sub> and (b) **ZnPF**<sub>Me</sub> in benzonitrile calculated according to Scheme 2. The ground-state absorption spectra of the dyads are shown as dotted lines.

#### Scheme 2



Finally, a kinetic scheme for the photoinduced processes in benzonitrile is presented in Scheme 2, where solid lines represent the major reaction path, dotted lines represent possible but minor reactions, and dashed lines present reactions which are nonresolved in time.

From the energetic point of view, the excited-state energies of the Zn and metal-free DA dyads are close to one another, which does not hold for the energies of the CT states. The energies of the CT state for the Zn compounds are about 0.2 eV lower compared to those of the metal-free derivatives.<sup>24</sup> This

(24) Johnson, D. G.; Svec, W. A.; Wasielewski, M. R. *Isr. J. Chem.* **1988**, 28, 193.

enhances the probability of the CT formation for the metalated DA complex in nonpolar solvents, even if the corresponding metal-free derivative undergoes CT only in solvents of high or moderate polarity. In the present case, the Zn dyad did not exhibit photoinduced electron transfer in toluene. This can be understood in the frame of the discussed model. For the studied compounds, the CT state was formed from the exciplex and the relative energy of the exciplex compared to that of the CT state governs the electron transfer.

The energy transfer has been found to be an important process in the photochemistry of the porphyrin-fullerene dyads.<sup>3</sup> In the present study, the rate of the energy transfer was  $\sim 10$  times as high as that determined for the porphyrin-fullerene dyad, i.e.  $\sim 4 \times 10^{12} \text{ s}^{-1}$  for **ZnPfMe** vs  $\sim 5 \times 10^{11} \text{ s}^{-1}$  for the Zn-porphyrin- $\text{C}_{60}$  dyad.<sup>3</sup> This can be explained by the energy gap between the singlet excited states of the phytochlorin and  $\text{C}_{60}$  chromophores, which is smaller than the gap between the corresponding states of the fully conjugated porphyrin and  $\text{C}_{60}$  chromophores.

Another significant difference between the phytochlorin- $\text{C}_{60}$  dyads and the porphyrin- $\text{C}_{60}$  dyads reported in refs 3 and 5 is the mechanism of the formation of the CT state. In the present study, an exciplex was observed as a precursor of the CT state, whereas in the case of the porphyrin- $\text{C}_{60}$  dyads,<sup>3,5</sup> the exciplex was not formed or not observed, probably because of lower time resolution. Recently, an exciplex was proposed, but not experimentally proved, to explain the photochemical behavior of the free-base porphyrin- $\text{C}_{60}$  dyad in THF,<sup>25</sup> and it was not clear whether it was followed by the CT state formation or not. The reason for the exciplex formation in phytochlorin- $\text{C}_{60}$  dyads can be the presence of a conformer, in which the chromophores are in a closer proximity to one another. The close proximity of the chromophores was not possible for the porphyrin-fullerene dyad, because of the presence of four phenyl groups in the porphyrin moiety. Even slower electron-

transfer rates ( $< 2 \times 10^9 \text{ s}^{-1}$ ) were observed by Sakata et al.<sup>5</sup> for porphyrin-fullerene dyads, where the porphyrin donor was linked to the fullerene acceptor by a longer spacer group and the close proximity between the donor and acceptor was sterically hindered by the bulky *tert*-butyl groups of the porphyrin. The only paper reporting electron-transfer rates comparable to those observed by us is that of Michel-Beyerle et al.,<sup>26</sup> who studied the electron transfer between porphyrin and benzoquinone, covalently linked to form a sandwich-like structure. Thus, it seems that fast electron transfer takes place through the space, whereas the slow process occurs through the bond.

The charge recombination rate constants are compatible in all of the cases,  $k_{\text{ctg}}$  for **ZnPfMe** being  $\approx 4.8 \times 10^{10} \text{ s}^{-1}$  and for the Zn porphyrin-fullerene dyad  $2 \times 10^{10} \text{ s}^{-1}$ .

In the present study, the phytochlorin donor is excited to the second singlet state. More than half of the excited molecules undergo a fast ( $< 200 \text{ fs}$ ) conversion to the exciplex, and a smaller part relaxes to the first singlet excited state of the phytochlorin moiety. The latter relaxes to the exciplex with a time constant in the 2–50 ps time domain, which is accessible experimentally. A straightforward elimination of the role of the second singlet excited state in the exciplex formation would require excitation of the dyad to the first singlet state. This was not yet possible by the present laser system.

## 5. Conclusions

This study shows that the formation of the photoinduced charge-transfer state of the phytochlorin-fullerene dyad proceeds via the formation of an intramolecular exciplex in polar solvents such as benzonitrile. In nonpolar solvents the exciplex is formed but relaxes directly to the ground state without the formation of the charge-transfer state.

**Acknowledgment.** The work was supported by the Academy of Finland, the National Research Program, and the Technical Development Centre of Finland, the Nanotechnology Program.

JA9915605

(25) Imahori, H.; Ozawa, S.; Ushida, K.; Takahashi, M.; Azuma, T.; Ajavakom, A.; Akiyama, T.; Hasegawa, M.; Taniguchi, S.; Okada, T.; Sakata, Y. *Bull. Chem. Soc. Jpn.* **1999**, 72, 485.

(26) Häberle, T.; Hirsch, J.; Pöllinger, F.; Heitele, H.; Michel-Beyerle, M. E.; Anders, C.; Döhling, A.; Krieger, C.; Ruckemann, A.; Staab, H. A. *J. Phys. Chem.* **1996**, 100, 18269.